

Abstract

An *in situ* study was designed to investigate naturally developed demineralisation in human enamel in a widely non-destructive manner in combination with X-ray microtomography. Samples of human enamel were carried in the oral cavity of participants for 24 hours daily for either 21 or 29 days using so-called intraoral mandibular appliances (ICTs). Demineralisation was thereby generated in a natural way without causing caries in the subjects' dentition. By employing synchrotron-based X-ray microtomography (XMT) in combination with volume image analysis, a quantification and three-dimensional visualisation of different stages of mineral density loss was possible. Basic features of the demineralized samples were similar to those reported in earlier *in vitro* studies. However, the analysed samples showed significant differences in the morphology of surface attack and the degree of mineral density loss depending on the carrier, the exposure time and the position within the ICT. In particular, the varying local conditions within a carrier's oral cavity seem to be different than in an *in vitro* study. Our results show that the combination of ICTs and quantitative image analysis applied to XMT data provides an analytical tool which is highly suited for the fundamental investigation of naturally developed demineralisation processes.

Keywords: caries, mineral concentration, intraoral appliance, intra-oral cariogenicity test system, synchrotron radiation, quantitative image analysis.

1. Introduction

Several studies attempting to understand the kinetics of early demineralisation which starts underneath the enamel surface have been performed in the past. Imaging techniques such as optical microscopy (Darling, 1958) and electron microscopy (Haikel et al., 1983; Hicks and Silverstone, 1985; Jones and Boyde, 1987; Pearce and Nelson, 1989; Shellis and Hallsworth, 1987; Boyde et al., 1995, 1999) were frequently used. Those techniques have the disadvantage of penetrating the material under study a few nanometres to 1 μm only. Therefore, the resulting two-dimensional images provided a limited insight into the lesion development and required invasive tissue preparation for the investigation of structural changes below the surface of the specimens (Baumgartner et al., 2000).

An alternative approach is the application of X-ray micro computed tomographic (XMT) techniques which provide three-dimensional images of the scanned specimen. Numerous articles are reporting on enamel demineralisation using high resolution computed tomography have been published which (e.g., Bing He et al., 2011; Hamba et al., 2011; Schwass et al., 2009; Tanaka et al., 2010). Frequently synchrotron radiation is employed for XMT in order to achieve higher spatial resolution and contrast (Bonse and Busch, 1996). At a synchrotron light source the available photon flux density (Photons/ mm^2/s) is orders of magnitude higher and the beam propagation is quasi parallel. The latter allows for extending the distance between source and sample up to several 100 m. Consequently, unlike in conventional radiography which is based on X-ray tubes, the influence of the finite X-ray source on the image resolution is suppressed (cf., e. g., Rack et al., 2008). Furthermore, the high flux allows the use of monochromators. Monochromatic radiation increases the contrast while reducing beam-hardening artefacts (Brooks and Di Chiro, 1976).

Today, X-ray microtomography (XMT) is a mature technique with high potential for dental research (Delbem et al., 2009). Working in absorption contrast, the images acquired with (quasi-) monochromatic radiation allow for a quantitative measure of changes in the degree of demineralisation inside, e.g., enamel tissue. Several studies attempting to understand the three dimensional kinetics of demineralisation have been performed using XMT (Kernen et al., 2008; Kinney et al., 1994, 1995; Anderson and Elliott, 2000; Stock et al., 2003; Farah et al., 2009; Huang et al., 2007; Dowker et al., 2006; Delbem et al., 2009; Mitropoulos et al., 2010; Tafforeau and Smith, 2007; Dowker et al., 2003; Davis and Wong, 1996; Dowker et al., 2004; Elliott

et al., 1994), even though extrapolating the three-dimensional de- and remineralisation processes from such a measurement is a non-trivial task (Dowker et al., 2003).

Some studies found in the literature are based on *in vitro* investigations, i.e. the demineralisation is artificially produced outside the oral cavity. Obviously, the clinical relevance of *in vivo* studies is significantly higher, in particular due to the multi-factorial nature of dental caries (ten Cate, 1994; Zero, 1995). Unfortunately, XMT is inapplicable for human dental *in vivo* studies for multiple reasons. One reason is the high mutagen potential of the employed hard X-ray radiation. Hence, demineralised teeth have to be extracted prior to imaging (Dowker et al., 2004, Huang et al., 2007, 2010). This makes time-resolved investigations of demineralisation processes impossible. Furthermore, information on the duration of and the conditions during demineralisation is limited.

As an alternative, we propose an *in situ* study using intraoral appliances (intra-oral cariogenicity test systems, ICT) which allow for an exposure of enamel samples to the human oral cavity over longer periods of time. Consequently, they represent promising tools to study naturally developed demineralisation in human oral cavities without causing any decay of the natural dentition (Koulourides and Volker, 1964, Koulourides and Chien, 1992). Thus, *in situ* studies combining ICTs with XMT imaging of the demineralised samples may bridge the gap between the highly controlled laboratory condition *in vitro* and the uncontrolled clinical situation *in vivo*. It is the aim of our pilot study to test the applicability of these techniques for the investigation of natural demineralisation processes. To the best of our knowledge such studies have not been performed so far. Of particular interest is whether the enamel demineralisation differs in its morphology from artificially generated lesions.

Furthermore, commonly earlier studies focused mainly on the evaluation the three-dimensional (3D) image data by means of volume renderings and density profiles along line sections. In our work methods from quantitative volume image analysis are introduced. Their application allows one to fully exploit the information provided by the 3D image data.

2. Materials and Methods

2.1. Preparation of specimens and intraoral appliance

Eight caries free third molars were extracted and stored for 24 h in Ringer's solution (DAB 7; Delta-Pharma, Pfullingen, Germany). After extraction the remaining tissue was removed with a scalpel under running water. With a diamond-coated wire saw (wire: 300 µm; saw: Type 4240, Well, Mannheim, Germany) the crowns were separated from the roots. During the sawing process the teeth were wetted constantly with phosphate enriched Na-Cl solution. 33 cubes of roughly 1 mm³ volume consisting of enamel of the occlusal surfaces and parts of contiguous dentine were prepared.

The specimens were covered with a varnish coat on five faces, leaving only the natural outer (occlusal) enamel surface free (Nail varnish: Nivea, Beiersdorf, Hamburg, Germany). The cubes were sterilised for 25 min at 1.8 bar and 122 °C (Technoclav 50, Technomara, Fernwald, Germany).

Afterwards 32 samples were randomly integrated into four removable ICTs, as shown in Fig. 1. The assembled samples were covered with a gold-micro mesh that allowed for accumulation of plaque on the specimen surface.

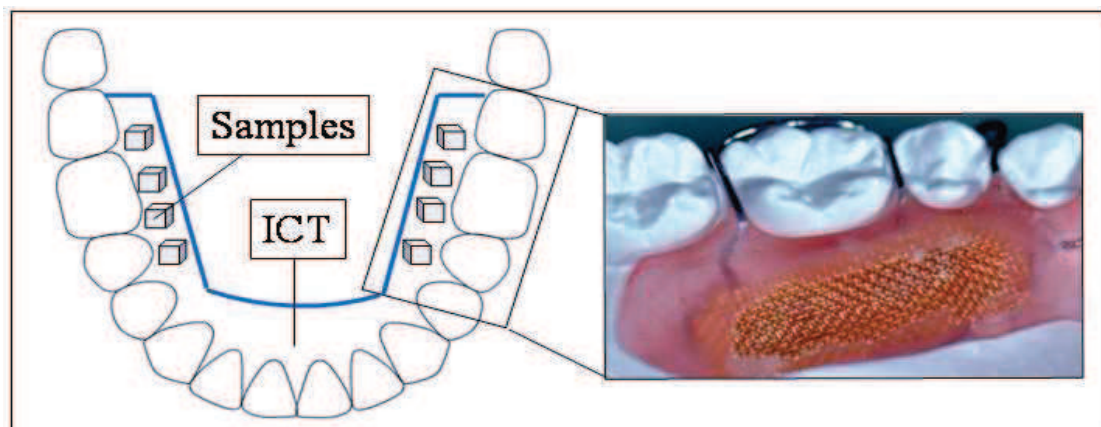


Fig. 1: Design of the intraoral mandibular appliances (ICT). The removable appliance is designed for the mandibular jaw. On the lingual side of the 3rd and 4th quadrand four samples of human enamel are polymerised below the micromesh (photograph).

2.2. Participants and experimental setup

Four participants volunteered for the pilot-study (3 female, 1 male, age: 23-27 years). The participants signed appropriate information consent forms. They were in good general health, had no infectious diseases and did neither take antibiotics nor medications that affect salivary flow for at least twelve months before and during the study. All participants were non-smokers and had moderate past caries experience with restored decays. If necessary, radiographs were taken to exclude caries and all

carious lesions were restored by a dentist of the Department of Conservative and Preventive Dentistry, RWTH Aachen University, Germany. The participants had a minimum of 28 natural teeth and generally good periodontal health. They wore the ICT day and night and removed it only for individual oral hygiene with fluoride toothpaste and to clean the ICT twice a day with fluoride-free toothpaste. To allow plaque to grow under the micro mesh the participants were instructed to clean the area of the specimens only by using running water. We chose different time periods of carrying the samples, presuming demineralisation to emerge after a period of at least three and at most four weeks. Since the time period for the XMT measurement was constricted to several hours during one day, all samples had to be removed from the ICTs on the same day. Therefore, two research subjects (participants A and B) started with the *in situ* study 21 days and two subjects (participants C and D) 29 days before the day of measuring. After extraction and during XMT measurement each sample was stored in a labelled closed container filled with Ringer's solution. A total of seven samples from participant A, eight from participant B, seven from participant C and one from participant D were scanned by XMT.

2.3. Synchrotron-based microtomography using hard X-rays

The XMT measurements were carried out at the BAMline, the first hard X-ray beamline of the BESSY-II light source (Helmholtz Zentrum für Materialien und Energie, Berlin, Germany, cf. Rack et al., 2008b). Quasi-monochromatic radiation of 25 keV X-ray photon energy was attained by setting a double-multilayer monochromator (approximately 1% energy bandwidth). Attenuators were inserted to block photons passing the monochromator by means of total reflection. To convert the synchrotron light after transmitting the sample into visible light, a 7- μm -thick YAG:Ce (Ce-doped $\text{Y}_3\text{Al}_5\text{O}_{12}$) single-crystal scintillator was used. The scintillator was coupled via diffraction-limited visible light optics to a CCD camera (VersArray: 2048B, 2048 \times 2048 pixel, Princeton Instruments). The indirect detector samples the visible light image with 1.6 μm effective pixel size. The spatial resolution achieved is approximately 7-8 μm . The images were taken in absorption mode, i.e. the detector was placed close downstream of the samples, which allows for neglecting coherence effects on our results, i.e. X-ray inline phase contrast. Each specimen was scanned with 900 projections over a 180° rotation. Three-dimensional data sets were reconstructed using the filtered backprojection algorithm (Kak and Slaney, 1988)

implemented in the software package PyHST of the SciSoft group of the European Synchrotron ESRF (Banhart, 2008; Mirone et al., 2012).

2.4. Image analysis

Tomographic reconstruction yields volume image data represented as a three-dimensional matrix of grey values. In our case, each point in this matrix (a three-dimensional pixel which is called voxel) corresponds to $(1.6 \mu\text{m})^3$ of material. Our image analysis is based on the assumption that the value associated with each voxel is approximately proportional to the local attenuation coefficient (LAC) of the material which is directly connected to its local physical density. Dowker et al., 2003 introduced a method for the reconstruction of the mineral concentration from the LAC modelling enamel as a two-phase system. Since the parameters of this model are unknown an uncertainty is introduced into the analysis results.

In this article, an alternative approach is proposed. Making sure that sound (non-demineralised) enamel is always included in the image we can normalise and therefore measure the relative density loss due to demineralisation in a quantitative manner (Rack et al., 2008a).

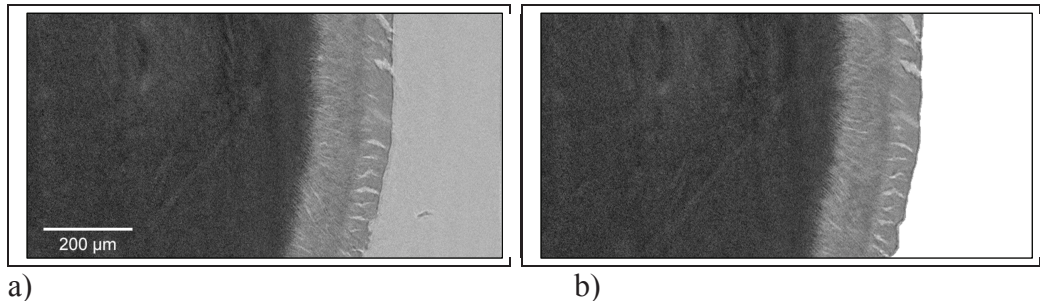


Fig. 2. Sectional images of the original grey value image (a) and the original image masked with reconstructed surface (b) for sample C1.

In a first step, relevant regions were cropped from the volume images. After denoising the resulting images by application of a 3x3x3 mean-filter, they were binarised using a simple threshold. The exposed enamel surface was identified by a morphological closure (Ohser and Schloditz, 2009). The distance of each enamel voxel to the sample surface was computed using the Euclidean distance transform. This transform determines for each foreground (enamel) voxel the distance to the closest background (liquid) voxel (Ohser and Schloditz, 2009). Finally, for all voxels with the same distance value the grey values in the original image were counted. Hence, the distribution of grey values, i.e. the degree of demineralisation, for points with a given distance to the surface was investigated. For processing and analysis of

the volume images we used the MAVI software package (MAVI, 2012). Sectional images of an original image and the reconstructed surface are shown in Fig. 2.

3. Results

Representative cross sections and renderings of the reconstructed grey value images of three samples showing different degrees of demineralisation are shown in Fig. 3. Samples worn by participants A and B, which were extracted after 21 days, showed an intact surface and no or very mild stages of sub-surface demineralisation (Fig. 3a). The samples from participants C and D were extracted after 29 days. All seven samples from participant C (e.g., Fig. 3b) showed different gradual changes in the enamel structure. Seven samples worn by participant D were disintegrated to a degree which made structural investigation impossible. Only one sample remained stable enough to be scanned (sample D4, Fig. 3 c). In this sample, demineralisation occurred in form of a deep demineralisation zone which partially fractured thus forming large subcutaneous cavities. The original sample surface was completely destroyed.

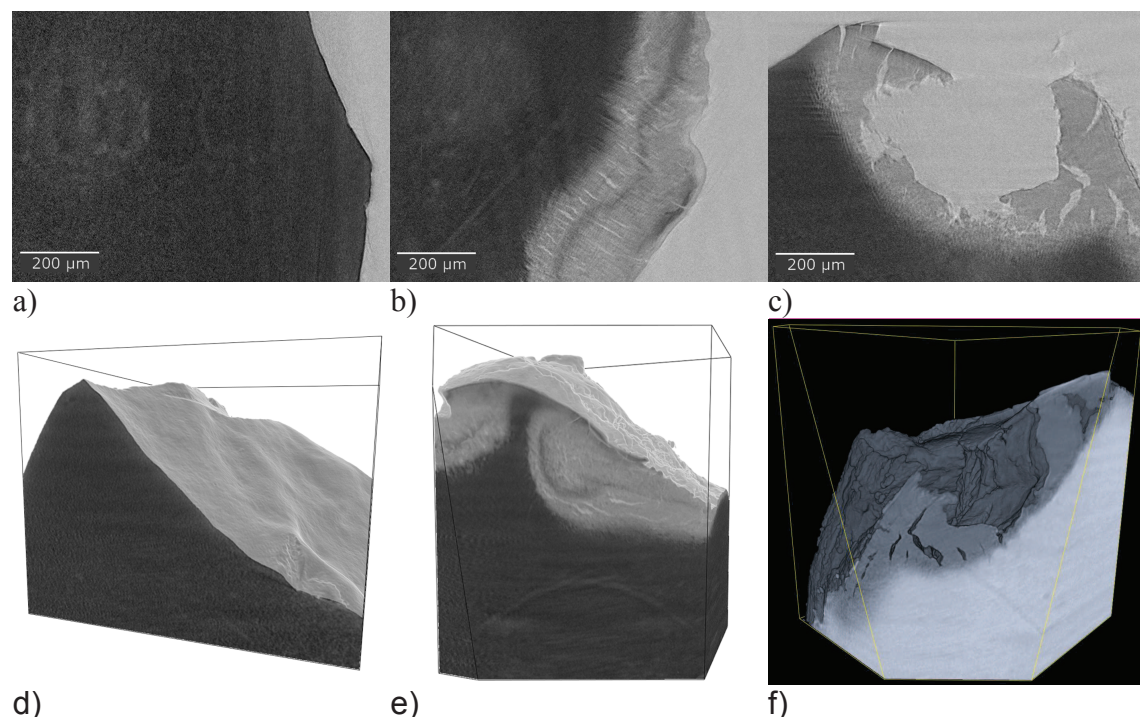


Fig. 3. Representative cross section images and volume renderings showing mild sub-surface demineralisation (a, d: sample B4), intermediate (b, e: sample C3) and severe (c, f: sample D4) stages of demineralisation.

The images were analysed using the image processing techniques described above. Since all samples worn by participants A and B showed a similar structure, only one sample for each of these participants was included in the analysis. For participant C, one sample was excluded from the analysis due to inappropriate sample geometry. The remaining six samples were analysed. For the remaining sample of participant D, a morphological reconstruction of the sample surface was not possible.

Fig. 4 shows the mean relative grey value (the mean grey value in a given depth divided by grey value for sound enamel) as a function of the distance to the reconstructed sample surface. Since mean grey values for consecutive distance values varied to a certain degree a smoothing spline was fit to the observations to obtain the curves shown in Fig. 4. Bright areas close to the sample surface (see e.g. Fig. 2 or Fig. 3 a) were partly levelled out by this procedure.

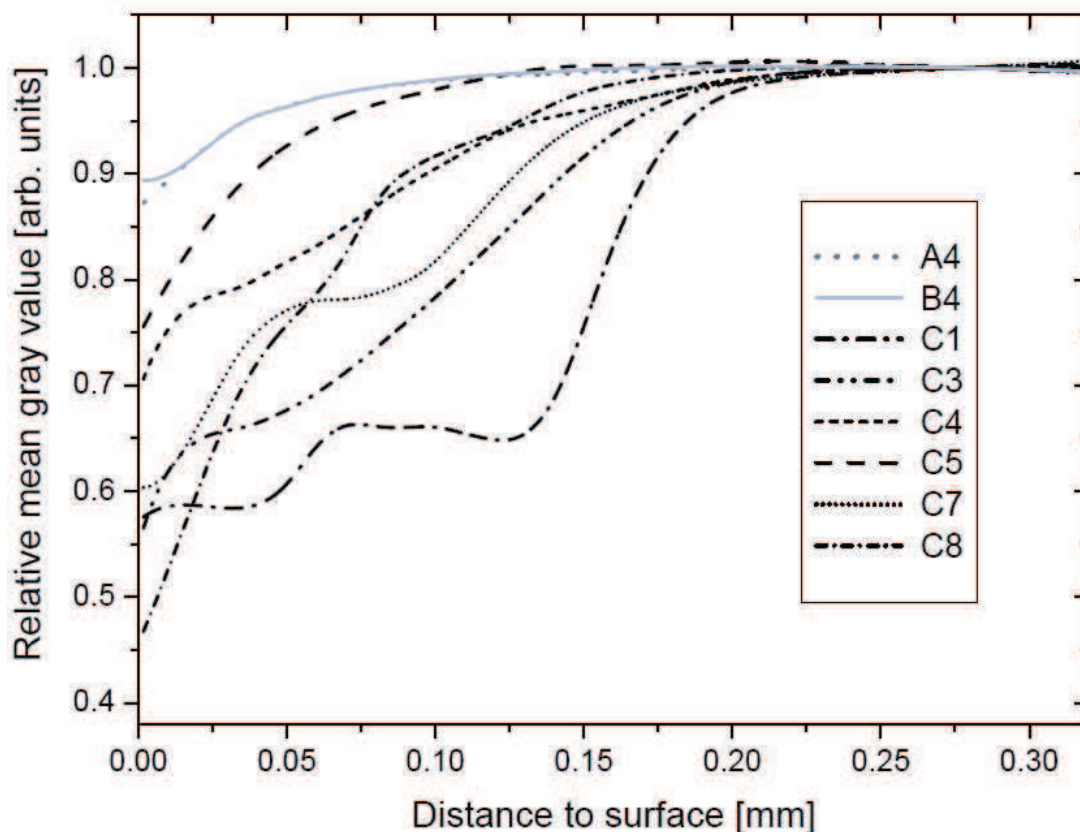


Fig. 4. Relative mean grey value (mean grey value divided by grey value for sound enamel) as a function of the distance to the sample surface. High grey values correspond to high enamel density; lower grey values indicate demineralisation of the material. Subjects A and B exposure time 21 days, C 29 days.

In the plots, a value of one corresponds to sound enamel. The difference from one can be used as a measure for the degree of demineralisation of the sample. Ring

artefacts, which are a common type of artefacts in tomographic image data (see Fig. 3 e or Fig. 5 b below), only appeared at relatively large distances to the demineralised zone such that they did not affect the analysis.

Further results of the analysis are summarized in Table 1. In this table the depth of demineralisation is defined as the minimal distance to the sample surface such that the relative mean grey value shown in Fig. 4 reaches the value of 1.

Table 1

Degree and depth of demineralisation for the analysed samples

Sample	Analysed volume [voxel]	Maximal reduction of mean grey value [%]	Depth of demineralisation [μm]
A4(1d)	738 x 783 x 1053	12.4	201
B4(2d)	747 x 955 x 1040	9.5	158
C1(3a)	453 x 330 x 666	42.1	267
C3(3c)	571 x 579 x 772	43.4	243
C4(3d)	721 x 552 x 490	32.4	252
C5(3e)	580 x 227 x 453	25.6	135
C7(3g)	693 x 533 x 542	40.0	269
C8(3h)	542 x 736 x 748	51.5	210

The results show significant differences in tissue loss between different exposure times and carriers. However, also in samples worn by the same person for the same period differences in degree and morphology of the demineralisation were observed. To further illustrate these differences, Fig. 5 shows volume renderings of samples C1 and C4. Sample C1 shows a well-organized progress of demineralisation which can be divided into two zones at different depth separated by a bright intermittent layer of almost full mineral density which is located approximately 100 μm below the enamel surface. In addition to the obvious loss of mineral density subcutaneous porosities were observed in the form of elongated pores which extend perpendicular to and approximately 100-200 μm underneath the enamel surface.

Contrary, the acid-attack on sample C4 is more localised. Areas with deeply penetrating demineralisation alternate with areas with only mild stages of demineralisation. Note that this local attack results in a comparably low degree of demineralisation as measured by the volume image analysis and shown in Fig. 4 for this sample. Highly demineralised areas show a similar layer structure as the homogeneous sample C1. However, the amount of subcutaneous pores in this sample is much lower than in sample C1.

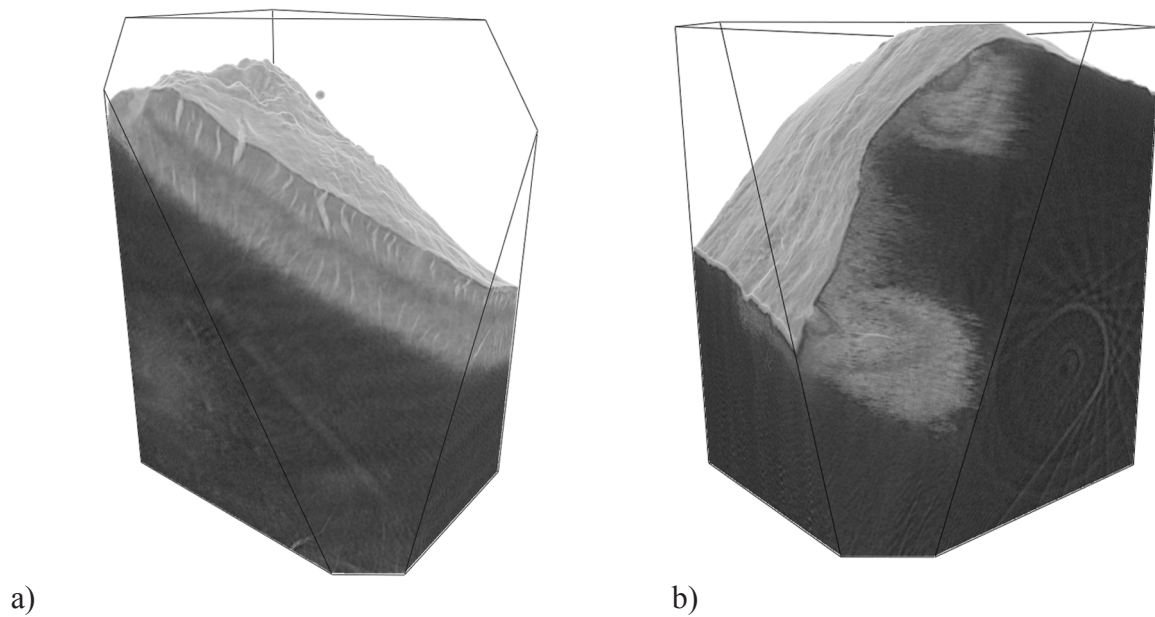


Fig. 5. Visualisation of samples, C1 (a) ($0.72 \times 0.53 \times 1.07 \text{ mm}^3$) and C4 (b) ($1.15 \times 0.88 \times 0.78 \text{ mm}^3$). The different morphology of surface penetration is clearly visible. Imaging artefacts (half-circles) due to detector inhomogeneities are present in (b).

4. Discussion & Conclusion

The aim of this pilot-study is to introduce a protocol for studying demineralisation in human enamel *in situ*. For the latter, intraoral mandibular appliances have been successfully applied.

In our study, zones of the incipient enamel lesions including defined surface layers were observed. The zones exhibited the characteristics of natural caries and might be similar to the classical zones described by Darling and Gustafson (Darling, 1956, 1958; Gustafson, 1957). Therefore, the morphology of *in situ* demineralised enamel would be equivalent to *in vitro* developed lesions (Zero, 1995).

The observed demineralisation differed significantly in grade, depth and morphology due to different carrying periods as well as non-equal conditions in the participants' oral habitat. In samples with progressed demineralisation, two types of corrosive attack – planar surface attack or pitting – were observed. Both types showed signs of an intermittent layer approximately $100 \mu\text{m}$ below the deepest demineralization front. This layer has a high concentration in mineral almost matching the density of the intact enamel. Yet, the X-ray images contain no information about whether this layer is a solid barrier or the accumulation of corrosion products (mainly dissolved Ca^{2+} ions) in the liquid. Tubular porosity was found in the demineralisation zones of many

samples in this study whereby the radial orientation of the pores most likely follows the patterning of the enamel crystalline rods in the corresponding zone.

From our observation on the samples exposed for 29 days we postulate a four-layer structure of demineralization: close to the enamel surface, demineralization creates a layer of strongly reduced density marking the beginning decay. At ~ 100 μm depth a higher density layer is observed followed by another porous low density layer. The final fourth layer is formed by sound enamel. Due to the averaging properties of the employed volume analysis algorithm, the intermittent zone between the two demineralisation layers which is visible in the images did not show up as clearly in the density profiles in Fig. 4.

It is well established that the lesion development depends on different individual factors, e.g., salivary rate, mineral concentration of the salivary, buffering capacity and nutrition behaviour (Silverstone et al., 1988). Under certain *in vivo* conditions a demineralisation can even stagnate, or furthermore regress in terms of remineralisation (Robinson, 2009). Significant differences in demineralisation, in particular between participants C and D, were also found in our study. However, due to the small number of research subjects, a detailed investigation of the influence of individual factors was not possible. For this purpose, it is desirable to perform a study including a much larger number of research subjects with differing individual conditions. Besides the progress of demineralisation, the remineralising role of fluoride in caries prevention in human subjects can be studied in a precise way. A detailed analysis of *in situ* remineralisation of enamel will be the topic of our future research.

Due to insufficient information on the development of natural demineralisation processes, it was found challenging to select the optimal point in time for sample removal. Two different carrying periods were selected assuming that demineralisation occurs after at least two and at most four weeks. Additionally, only a single time window was available for the XMT measurements such that the *in situ* part of our study had to be completed up to a hard deadline. Our results show that a period of three to four weeks is a critical time window for start and development of demineralisation processes and seems to be most suited for sample removal. For future studies, it is advisable to remove samples at multiple time points in order to follow the demineralisation process in different individuals. Even a reintegration of scanned samples into the ICT can be considered.

5. Summary

We have presented a pilot study aiming at the development of a protocol which allows for the investigation of natural demineralisation processes in human enamel. For this purpose, enamel samples were inserted in the oral habitat of four research subjects using ICTs. After a certain carrying period, the samples were scanned by XMT and the degree of demineralisation was quantified using methods from 3D image analysis.

The ICT was found to be an instrument well-adapted for the investigation of *in situ* development of naturally demineralised enamel. The chosen dimension of the samples was well suited for fitting into the ICTs and subsequently into the XMT detector's field of view. ICTs provided environmental conditions for natural plaque formation on the sample surface without causing decay on the participants' dentition. Access of dietary substrate and salivary was given, which resulted in plaque accumulation that led to a diagnosable demineralisation.

Synchrotron XMT provided highly resolved images clearly showing the density variations within the enamel structure. Methods from quantitative image analysis do not only allow for a visualisation but also for a quantification of the degree of demineralisation in different samples. In contrast to classical two-dimensional imaging techniques, XMT captures the fully three-dimensional morphology of the demineralised areas. Furthermore, the degree of demineralisation in a given distance to the true (typically non-planar) sample surface can be investigated in a three-dimensional manner.

Acknowledgements

The authors would like to thank Dr. A. Haibel and Dr. I. Manke (Hahn Meitner Institute, Berlin, Germany) as well as Dr. H. Riesemeier (Federal Institute of Materials Research and Testing (BAM), Berlin, Germany) for their support and suggestions during the experiments as well as for discussion. Beamtime at the BAMline was provided by the BESSY II light source (Helmholtz-Zentrum Berlin, Germany). Special thanks go to Maximilian Lautensack, Aglaia Rack, Elina Redenbach.

References

- Anderson, P., Elliott, J.C., 2000. Rates of mineral loss in human enamel during in vitro demineralisation perpendicular and parallel to the natural surface. *Caries Res.* 34, 33–40.
- Banhart, J., 2008. *Advanced Tomographic Methods in Materials Research and Engineering*. Oxford University Press.
- Baumgartner, A., Dichtl, S., Hitzenberger, C.K., Sattmann, H., Robl, B., Moritz, A., Fercher, A.F., Sperr, W., 2000. Polarization-sensitive optical coherence tomography of dental structures. *Caries Res.* 34, 59–69.
- Bing, H., Shengbin, H., Chaoliang, Z., Junjun, J., Yuqing, H., Liying, X., Xuedong, Z., 2011. Mineral densities and elemental content in different layers of healthy human enamel with varying teeth age. *Arch. Oral. Biol.*, Mar 14, 2011. [Epub ahead of print].
- Bonse, U., Busch, F., 1996. X-ray computed microtomography (μ CT) using synchrotron radiation (SR). *Prog. Biophys. Molec. Biol.* 65, 133-169.
- Boyde, A., Davy, K.W.M., Jones, S.J., 1995. Standards for mineral quantification of human bone by analysis of backscattered electron images. *Scanning.* 17, 6-7.
- Boyde, A., Travers, R., Glorieus, F.H., Jones, S.J., 1999. The mineralization density of iliac crest bone from children with osteogenesis imperfect. *Calcif Tissue Int.* 64, 185-190.
- Brooks, R. A. and Di Chiro, G., 1976. Beam hardening in X-ray reconstructive tomography. *Phys. Med. Biol.* 21, 390-398.
- Buzug, T.M, 2008. *Computed Tomography. From Photon Statistics to Modern Cone-Beam CT*. Springer Verlag, Heidelberg, Germany. ISBN: 978-3-540-39407-5.
- Darling, A.I., 1956. Studies of the early lesion of enamel caries with transmitted light, polarised light and radiography. *Br. dent. J.* 101, 289- 299.
- Darling, A.I., 1958. Studies of the early lesion of enamel caries. Its nature, mode of spread and points of entry. *Br. dent. J.* 105, 119-135.
- Davis, G.R., Wong, F.S., 1996. X-ray microtomography of bones and teeth. *Physiol. Meas.* 17, 121–146.
- Delbem, A.C.B., Sassaki, K.T., Vieira, A.E.M., Rodrigues, E., Bergamaschi, M., Stock, S.R., Cannon, M.L., Xiao, X., De Carlo, F., Delbem, A.C.B., 2009. Comparison of methods for evaluating mineral loss: Hardness versus synchrotron microcomputed tomography. *Caries Res.* 43, 359–365.
- Di Masi, E., 2005. Synchrotron imaging of biominerals highlights new results and challenges. *Synchr. Rad. News.* 18, 17–22.

- Dowker, S.E.P., Elliott, J.C., Davis, G.R., Wilson, R.M., Cloetens, P., 2004. Synchrotron X-ray microtomographic investigation of mineral concentrations at micrometre scale in sound and carious enamel. *Caries Res.* 38, 514–522.
- Dowker, S.E.P., Elliott, J.C., Davis, G.R., Wassif, H.S., 2003. Longitudinal study of the three-dimensional development of subsurface enamel lesions during in vitro demineralization. *Caries Res.* 37, 237–245.
- Farah, R.A., Swain, M.V., Drummond, B.K., Cook, R., Atieh, M., 2009. Mineral density of hypomineralised enamel. *J. Dentist.* 38, 50–58.
- Gustafson, G., 1957. The histopathology of caries of human dental enamel. With special reference to the division of the carious lesion into zones. *Acta. Odontol. Scand.* 15, 13–55.
- Hamba, H., Nikaido, T., Inoue, G., Sadr, A., Tagami, J., 2011. Effects of CPP-ACP with sodium fluoride on inhibition of bovine enamel demineralization: A quantitative assessment using micro-computed tomography. *J. Dent.* [Epub ahead of print].
- Haikel, Y., Frank, R.M., Voegel, J.C., 1983. Scanning electron microscopy of the human enamel surface layer of incipient carious lesions. *Caries Res.* 17, 1–13.
- Hicks, M.J., Silverstone, L.M., 1985. Internal morphology of surface zones from acid-etched caries-like lesions: a scanning electron microscopic study. *J. Dent. Res.* 64, 1296–1301.
- Hsieh, J., 2009. *Computed Tomography: Principles, Design, Artifacts and Recent Advances*, 2nd edn. SPIE., Bellingham.
- Huang, T.T., Jones, A.S., He, L.H., Darendeliler, M.A., Swain, M.V., 2007. Characterisation of enamel white spot lesions using X-ray micro-tomography. *J. Dent.* 35, 737–743.
- Huang, T.T., He, L.H., Darendeliler, M.A., Swain, M.V., 2010. Correlation of mineral density and elastic modulus of natural enamel white spot lesions using X-ray microtomography and nanoindentation. *Acta Biomater.* 6, 4553–4559.
- Jones, S.J., Boyde, A., 1987. Scanning microscopic observations on dental caries. *Scanning Microsc.* 1, 1991–2002.
- Kak, A.C., Slaney, M., 1988. *Principles of Computerized Tomographic Imaging*. IEEE Press, New York.
- Kernen, F., Waltimo, T., Deyhle, H., Beckmann, F., Stark, W., Müller, B., 2008. Synchrotron radiation-based micro computed tomography in the assessment of dentin de- and remineralization. *Proc. Of SPIE.* 7078, 1–9.
- Kielbassa, A.M., Schendera, A., Schulte-Mönting, J., 2000. Microradiographic and microscopic studies on in situ induced initial caries in irradiated and nonirradiated dental enamel. *Caries Res.* 34, 41–47.

Kinney, J.H., Marshall, Jr. G.W., Marshall, S.J., 1994. Three dimensional mapping of mineral densities in carious dentin: Theory and method. *Scanning Microsc.* 8, 197–205.

Kinney, J.H., Balooch, M., Haupt, Jr. D.L., Marshall, S.J., Marshall, Jr. G.W., 1995. Mineral distribution and dimensional changes in human dentine during demineralization. *J. Dent. Res.* 74, 1179-1184.

Koulourides, T., Volker, J.F., 1964. Changes of enamel microhardness in the human mouth, Alabama. *J. Med. Sci.* 1, 435–347.

Koulourides, T., Chien, M.C., 1992. The ICT in situ experimental model in dental research. *J. Dent. Res.* 71, 822–827.

Mirone, A., Wilcke, R., Hammersley, A., Ferrero, C., 2012. PyHST - High Speed Tomographic Reconstruction.
<http://www.esrf.eu/UsersAndScience/Experiments/TBS/SciSoft/>.

MAVI, 2012. Modular Algorithms for Volume Images, Fraunhofer ITWM,
www.mavi-3d.de.

Ohser, J., Schladitz, K., 2009. 3D Images of Material Structures. Wiley, Weinheim.

Pearce, E.I., Nelson, D.G., 1989. Microstructural features of carious human enamel imaged with backscattered electrons. *J. Dent. Res.* 68, 113–118.

Rack, A., Riesemeier, H., Zabler, S., Weitkamp, T., Müller, B.R., Weidemann, G., Modregger, P., Banhart, J., Helfen, L., Danilewsky, A.N., Gräber, H.G., Heldele, R., Mayzel, B., Goebbels, J., Baumbach, T., 2008a. The high resolution synchrotron-based imaging stations at the BAMline (BESSY) and TopoTomo (ANKA). *Proc. SPIE.* vol. 7078, 70780X-1– 70780X-9.

Rack, A., Zabler, S., Müller, B.R., Riesemeier, H., Weidemann, G., Lange, A., Goebbels, J., Hentschel, M., Görner, W., 2008b. High resolution synchrotron-based radiography and tomography using hard X-rays at the BAMline (BESSY II). *Nucl. Instr. Meth. Phys. Res. A.* 586, 327-344.

Robinson, C., Shore, R.C., Brookes, S.J., Strafford, S., Wood, S.R., Kirkham, J., 2000. The chemistry of enamel caries. *Crit. Rev. Oral. Biol. Med.* 11, 481–495.

Robinson, C., 2009. Fluoride and the caries lesion: interactions and mechanism of action. *Eur. Arch. Paediatr. Dent.* 10, 136-140.

Schwass, D.R., Swain, M.V., Purton, D.G., Leichter, J.W., 2009. A System of Calibrating Microtomography for Use in Caries Research. *Caries Res.* 43, 314-321.

Shellis, R.P., Hallsworth, A.S., 1987. The use of electron microscopy in studying enamel caries. *Scanning Microsc.* 1, 1109–1123.

Silverstone, L.M., Hicks, M.J., Featherstone, M.J., 1988. Dynamic factors affecting lesion initiation and progression in human dental enamel. The dynamics and nature of enamel caries. *Quintessenz Int.* 19, 683–710.

Stock, S.R., Ignatiev, K.I., Dahl, T., Veis, A., De Carlo, F., 2003. Three-dimensional microarchitecture of the plates (primary, secondary, and carinar process) in the developing tooth of *Lytechinus variegatus* revealed by synchrotron X-ray absorption microtomography (microCT). *J. Struct. Biol.* 144, 282–300.

Stock, S.R., 2008. *MicroComputed Tomography: Methodology and Applications*. CRC Press. London, New York, Boca Raton.

Tanaka, R., Shibata, Y., Manabe, A., Miyazaki, T., 2010. Micro-structural integrity of dental enamel subjected to two tooth whitening regimes. *Arch. Oral Biol.* 55, 300-8.

Zabler, S., Cloetens, P., Zaslansky, P., 2007. Fresnel-propagated submicrometer x-ray imaging of water-immersed tooth dentin. *Optics Lett.* 32, 2987-2989.

Zero, D.T., 1995. In situ caries models. *Adv. Dent. Res.* 9, 214–230.